Celest Mech Dyn Astr
DOI 10.1007/s10569-011-9353-3

ORIGINAL ARTICLE

Asymptotic solution for the two-body problem with constant tangential thrust acceleration

Claudio Bombardelli · Giulio Baù · Jesus Peláez

Received: 3 November 2010 / Revised: 7 April 2011 / Accepted: 3 May 2011

Abstract An analytical solution of the two body problem perturbed by a constant tangential acceleration is derived with the aid of perturbation theory. The solution, which is valid for circular and elliptic orbits with generic eccentricity, describes the instantaneous time variation of all orbital elements. A comparison with high-accuracy numerical results shows that the analytical method can be effectively applied to multiple-revolution low-thrust orbit transfer around planets and in interplanetary space with negligible error.

Keywords Two body problem · Tangential thrust · Asymptotic expansion · Orbit transfer

1 Introduction

Tangential thrust is an effective way of changing the instantaneous orbital energy of a spacecraft and has important implications in orbital dynamics. In the framework of the two-body problem for example, it is known that when constant acceleration is available the thrust strategy providing maximum increase (or decrease) of the *instantaneous* orbit semimajor axis consists of having the thrust vector pointed along the tangent to the orbit.[1]

Orbit raising, planetary escape and planetary capture maneuvers can be carried out with continuous tangential low thrust usually based on electric propulsion systems providing considerable fuel mass savings when compared to chemical options. Because of the relatively small magnitude of the available acceleration for these systems, a low tangential thrust maneuver typically involves multiple revolutions and relatively large thrust times which turn

[1] Note that the maximum increase in the orbital energy *over a fixed period of time* is obtained when the thrust is aligned with the primer vector minimizing the Hamiltonian associated with the optimum control problem. This does not generally coincide with the tangent to the orbit.

C. Bombardelli (✉) · J. Peláez
ETSI Aeronauticos, Plaza Cardenal Cisneros 3, Madrid, Spain
e-mail: claudio.bombardelli@upm.es

G. Baù
CISAS, Via Venezia 13, Padova, Italy

Published online: 19 June 2011

into a numerical burden when it is time to simulate the trajectory evolution or, to a larger extent, in the optimization phase of low-thrust mission design. For these reasons the problem of propagating a low tangential thrust trajectory using (approximate) analytical methods has been analyzed by many authors in the literature starting from the late 50s and continuing until recently. The goal has always been to find simple analytical models to provide fast and relatively accurate propagation of these types of low-thrust orbits. Benney (1959), first analyzes the problem of escaping from a circular orbit using tangential thrust, which is also dealt with by Boltz (1992) and later by Battin (1999). The extension to non-circular orbits is considered by Kechichian (1998) and by Gao and Kluever (2005) who use approximate solutions following the evolution of the averaged orbit equations of motion in Gauss form. An elegant asymptotic solution for the evolution of elliptic orbits of moderate eccentricity is also presented in a chapter of the book by Kevorkian et al. (1981).

The problem of all these proposed method is that each of them suffers from specific limitations. Early methods (Benney 1959; Boltz 1992; Battin 1999) can only deal with circular or almost circular orbits, which limits their applicability to realistic astrodynamics problems. On the other hand more recent methods (Kechichian 1998; Gao and Kluever 2005), which are able to deal with elliptic orbits, cannot reproduce the oscillatory variations of the orbital elements along each orbit. Such variations can be crucial when low thrust interplanetary orbits are propagated.

In this article we develop an approximate, yet accurate analytical model to represent the average *and* oscillatory time evolution of all orbital elements by exploiting the use of perturbation theory and of a non-singular variation of parameter formulation of the orbital dynamics.

The equations of motion for the tangential-thrust-perturbed two-body-problem are written using the special perturbation method developed by Peláez et al. (2007). This method has the advantage of a relatively compact and simple formulation of the equations of motion and is free of singularities (with the exception of the unusual case of rectilinear "impact orbits"). Similar formulations have been proposed in the literature (see for instance Mandrogel 2008).

Assuming the acceleration magnitude is small when compared to the local gravity (as reasonable given the limit of current low-thrust propulsion systems) we formulate the orbit dynamic problem as a general perturbation problem in which a small parameter, ε, represents the non-dimensional magnitude of the tangential acceleration. By a straightforward series expansion the first-order time evolution of the three generalized orbital elements associated to the planar orbital motion are obtained, in analytical close form, by simple quadrature. Secular and oscillatory terms are both computed, which are generally a combination of elliptic integrals of the first and second kind. Trigonometric series for the oscillatory terms are given in order to speed up the computation process. The effectiveness of the approximate analytical solution is tested for a transfer from GTO to Earth escape and from Earth to Mercury, in both cases assuming continuous and constant tangential acceleration and no orbit plane change.

2 Equations of motion

Let us consider a particle orbiting around a primary at initial radial position r_0 measured from the center of the primary and angular position θ_0 measured from the initial eccentricity vector. Let us employ, from now on, r_0 as the unit of distance and $1/\Omega_0$ as the unit of time where Ω_0 is the angular rate of a circular orbit with radius equal to the initial radius r_0

$$\Omega_0 = \sqrt{\frac{\mu}{r_0^3}},$$

with μ indicating the gravitational parameter of the primary.

The dimensionless angular momentum of the initial osculating orbit can be written, for later use as:

$$h_0 = \frac{\dot{\theta}_0}{\Omega_0} = \sqrt{1 + e_0 \cos\theta_0}. \tag{1}$$

Using the formulation described by Peláez et al. (2007), and under the hypothesis that all acting perturbation forces have a zero component along the normal to the orbital plane, the orbit geometry can be fully described by the three generalized orbital parameters:

$$q_1 = \frac{e}{h}\cos\Delta\gamma, \tag{2}$$

$$q_2 = \frac{e}{h}\sin\Delta\gamma, \tag{3}$$

$$q_3 = \frac{1}{h}, \tag{4}$$

where h is the dimensionless angular momentum of the osculating orbit, e its eccentricity and $\Delta\gamma$ is, for this particular case in which the orbit plane is constant, the rotation of the eccentricity vector with respect to the initial orbit.

From the above expressions the orbit eccentricity, the eccentricity vector rotation and the non-dimensional angular momentum can be written, for later use, as:

$$e = \frac{\sqrt{q_1^2 + q_2^2}}{q_3}, \tag{5}$$

$$\Delta\gamma = \tan^{-1}\left(\frac{q_2}{q_1}\right), \tag{6}$$

$$h = \frac{1}{q_3}. \tag{7}$$

The expression of the non-dimensional semimajor axis is then:

$$a = \frac{h^2}{1 - e^2} = \frac{1}{q_3^2 - q_1^2 - q_2^2}. \tag{8}$$

The independent variable used in the Peláez method is, again for the planar case, Peláez et al. (2007):

$$\theta = \nu + \Delta\gamma, \tag{9}$$

where ν is the true anomaly of the osculating orbit. Note that θ corresponds to the inertial angular position of the particle measured from the initial eccentricity vector.

A Sundmann transformation, corresponding to the angular momentum variation equation, relates θ to the dimensionless time t as:

$$\frac{d\theta}{dt} = \frac{h}{r^2} = q_3 s^2, \tag{10}$$

where s is the dimensionless transverse velocity of the particle and obeys (Peláez et al. 2007):

$$s = q_1\cos\theta + q_2\sin\theta + q_3. \tag{11}$$

The orbit radius as a function of the generalized orbital parameter can be obtained from the two equations above as:

$$r(\theta) = (q_3 s)^{-1} = \left(q_3^2 + q_1 q_3 \cos\theta + q_2 q_3 \sin\theta\right)^{-1}. \tag{12}$$

The evolution of the three generalized orbital parameters obeys (see Pérez et al. 2007):

$$\frac{d}{d\theta}\begin{pmatrix} q_1 \\ q_2 \\ q_3 \end{pmatrix} = \frac{1}{q_3 s^3}\begin{pmatrix} s\,\sin\theta & (s+q_3)\,\cos\theta \\ -s\,\cos\theta & (s+q_3)\,\sin\theta \\ 0 & -q_3 \end{pmatrix}\begin{pmatrix} a_r \\ a_\theta \end{pmatrix}, \tag{13}$$

where a_r and a_θ are, respectively, the component of the dimensionless perturbative acceleration along the instantaneous radial and transversal direction.

If the acceleration is always directed along the instantaneous velocity vector Eqs. (13) become:

$$\frac{d}{d\theta}\begin{pmatrix} q_1 \\ q_2 \\ q_3 \end{pmatrix} = \frac{\epsilon}{q_3 s^3\sqrt{e^2 + 2e\cos\nu + 1}}\begin{pmatrix} s\,\sin\theta & (s+q_3)\,\cos\theta \\ -s\,\cos\theta & (s+q_3)\,\sin\theta \\ 0 & -q_3 \end{pmatrix}\begin{pmatrix} e\sin\nu \\ 1 + e\cos\nu \end{pmatrix}, \tag{14}$$

where

$$\epsilon = \sqrt{a_r^2 + a_\theta^2} = \frac{A_t}{\mu/r_0^2} \tag{15}$$

is the corresponding dimensionless value of the constant tangential acceleration A_t. Note that, by use of Eqs. (5), (41), (9), (11), Eqs. (14) can be put in the form:

$$\frac{d\boldsymbol{q}}{d\theta} = \boldsymbol{F}(\boldsymbol{q}, \epsilon, \theta), \tag{16}$$

where $\boldsymbol{q} = (q_1, q_2, q_3)^T$ and $\boldsymbol{F}$ is a nonlinear vectorial function.

Equations (16) must be integrated with the appropriate initial conditions, namely:

$$\begin{aligned} q_1(\theta_0) &= e_0/h_0, \\ q_2(\theta_0) &= 0, \\ q_3(\theta_0) &= 1/h_0. \end{aligned}$$

3 Asymptotic solution

When considering high specific impulse electric propulsion systems, currently the most common low-thrust solution employed in space technology, typical values for the achievable acceleration with reasonable payload masses range around 100 mN/kg (Kemble 2006). In most circumstances (depending on the local gravity value for the particular orbit considered) the resulting dimensionless acceleration ϵ will also be a small quantity, and can be used to perform an asymptotic expansion of Eqs. (14) (and (10), which characterize, respectively, the trajectory geometry and its evolution in time.

3.1 Trajectory

In the hypothesis that ϵ is a small quantity we write the three generalized orbital elements as power series:

$$q_i(\theta, \epsilon) = q_{i0}(\theta) + \epsilon q_{i1}(\theta) + o(\epsilon) \quad i = 1...3 \tag{17}$$

Substituting into Eq. (16) , expanding in a Taylor series and solving for like powers of epsilon we obtain, for the zeroth order:

$$\frac{dq_{i0}}{d\theta} = 0,$$

showing that the zeroth order terms are just the (constant) generalized orbital elements of the unperturbed trajectory:

$$q_{10} = e_0/h_0, \tag{18}$$
$$q_{20} = 0, \tag{19}$$
$$q_{30} = 1/h_0, \tag{20}$$

where e_0 and h_0 are, respectively, the eccentricity and dimensionless angular momentum of the initial trajectory.

The differential equations for the first order terms results:

$$\frac{d}{d\theta}\begin{pmatrix} q_{11} \\ q_{21} \\ q_{31} \end{pmatrix} = \frac{h_0^3}{(1+e_0\cos\theta)^2\sqrt{e_0^2+2e_0\cos\theta+1}}\begin{pmatrix} e_0+2\cos\theta \\ 2\sin\theta \\ -1 \end{pmatrix}. \tag{21}$$

Equation (21) can be best integrated by introducing the new variable $\tilde{E}$ which obeys:

$$\tan\frac{\tilde{E}}{2} = \sqrt{\frac{1-e_0}{1+e_0}}\tan\frac{\theta}{2}. \tag{22}$$

Note that $\tilde{E}$, although similar, does not correspond to the eccentric anomaly of the osculating orbit, except when $\theta = \theta_0$ at the very beginning of the integration.[2] The following relations can be derived from Eq. (22):

$$\sin\theta = \frac{\sqrt{1-e_0^2}\sin\tilde{E}}{1-e_0\cos\tilde{E}},$$
$$\cos\theta = \frac{\cos\tilde{E}-e_0}{1-e_0\cos\tilde{E}},$$
$$\frac{d\tilde{E}}{d\theta} = \frac{1-e_0\cos\tilde{E}}{\sqrt{1-e_0^2}},$$

and substituted into Eqs. (21) yield:

$$\frac{dq_{11}}{d\tilde{E}} = \frac{h_0^3}{(1-e_0^2)^2}\frac{e_0(e_0^2-2)\cos^2\tilde{E}+2\cos\tilde{E}-e_0}{\sqrt{1-e_0^2\cos^2\tilde{E}}}, \tag{23}$$

$$\frac{dq_{21}}{d\tilde{E}} = \frac{h_0^3}{(1-e_0^2)^{3/2}}\frac{2\sin\tilde{E}(1-e_0\cos\tilde{E})}{\sqrt{1-e_0^2\cos^2\tilde{E}}}, \tag{24}$$

$$\frac{dq_{31}}{d\tilde{E}} = \frac{-h_0^3}{(1-e_0^2)^2}\frac{(1-e_0\cos\tilde{E})^2}{\sqrt{1-e_0^2\cos^2\tilde{E}}}. \tag{25}$$

[2] In such case θ and e_0 concide with the true anomaly and eccentricity of the osculating orbit, respectively.

Equations (23–25) can now be integrated. The full analytical solution, which for the cases of q_1 and q_3 involves elliptic integrals, are reported in Appendix I where series expansions are performed leading to the following compact form as a function of $\tilde{E}$:

$$q_{11}(h_0, e_0, \tilde{E}) = \frac{h_0^3}{(1-e_0^2)^2}[Q_{11}(e_0, \tilde{E}) - Q_{11}(e_0, \tilde{E}_0)], \tag{26}$$

$$q_{21}(h_0, e_0, \tilde{E}) = \frac{h_0^3}{(1-e_0^2)^{3/2}}[Q_{21}(e_0, \tilde{E}) - Q_{21}(e_0, \tilde{E}_0)], \tag{27}$$

$$q_{31}(h_0, e_0, \tilde{E}) = \frac{h_0^3}{(1-e_0^2)^2}[Q_{31}(e_0, \tilde{E}) - Q_{31}(e_0, \tilde{E}_0)]. \tag{28}$$

The analytical expressions for the functions $Q_{ij}(e_0, \tilde{E})$ are reported in Appendix I.

Once a first-order solution for the generalized orbital elements has been derived, Eq. (22) can be used to express all quantities as a function of the angular position θ desired. Finally, the radial position as well as the orbit eccentricity, semimajor axis and angular momentum can be derived through Eqs. (5, 7, 8, 12).

3.2 Time of flight

So far we have obtained the orbit characteristics as a function of the variables $\tilde{E}$ and θ. The last step is now to obtain the generalized orbital elements as a function of time so that the spacecraft position and velocity can be inferred at any given epoch.

The time t corresponding to a given θ for the perturbed trajectory can be conveniently written as a series expansion:

$$t(\epsilon, \theta) = t_0(\theta) + \epsilon t_1(\theta) + o(\epsilon), \tag{29}$$

where $t_0(\theta)$ correspond to the time of the unperturbed trajectory and the remaining part is the thrust-induced *phasing difference* between the perturbed and unperturbed trajectory:

$$\Delta t(\epsilon, \theta) = \epsilon t_1(\theta) + o(\epsilon).$$

By substituting Eq. (29) into Eq. (10) we obtain:

$$\frac{dt}{d\theta} = \frac{dt_0}{d\theta} + \epsilon \frac{dt_1}{d\theta} = \frac{1}{q_3 s^2}. \tag{30}$$

After substituting the expansions Eq. (17) into Eq. (30), expanding in a Taylor series and collecting terms of equal power of epsilon we obtain:

$$\frac{dt_1}{d\theta} = -\frac{q_{31}}{q_{30} s_0^3}(s_0 + 2q_{30}) - \frac{2q_{11}}{q_{30} s_0^3}\cos\theta - \frac{2q_{12}}{q_{30} s_0^3}\sin\theta, \tag{31}$$

where

$$s_0 = q_{10}\cos\theta + q_{30} = q_{30}(1 + e_0\cos\theta).$$

Equation (31) can be conveniently written with respect to the variable $\tilde{E}$ as:

$$\frac{dt_1}{d\tilde{E}} = \frac{3e_0 - (2 + 2e_0^2)\cos\tilde{E} + e_0\cos 2\tilde{E}}{q_{30}^4(1-e_0^2)^{5/2}} q_{11}(\tilde{E}) - \frac{2\sin\tilde{E} - e_0\sin 2\tilde{E}}{q_{30}^4(1-e_0^2)^2} q_{21}(\tilde{E})$$
$$- \frac{3 - (5e_0 - e_0^3)\cos\tilde{E} + e_0^2\cos 2\tilde{E}}{q_{30}^4(1-e_0^2)^{5/2}} q_{31}(\tilde{E}). \tag{32}$$

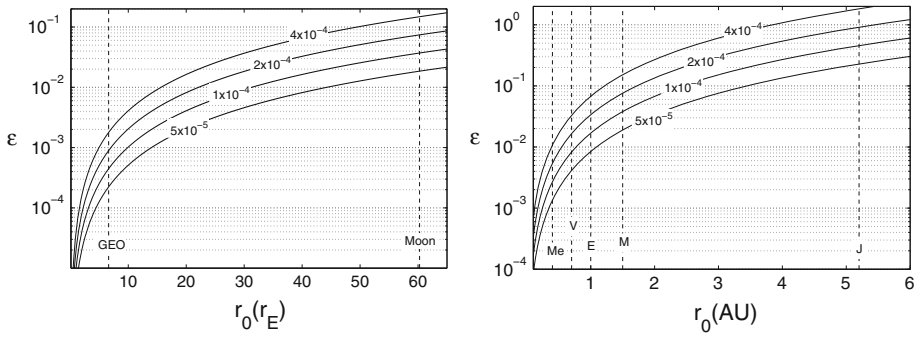

Fig. 1 Variability of the parameter epsilon for Earth (*right*) and interplanetary orbits (*left*)

The integration process is performed in Appendix II leading to the following compact form:

$$\Delta t(e_0, \theta) = \frac{\epsilon h_0^7}{(1-e_0^2)^{9/2}}[T(\tilde{E}) - T(\tilde{E}_0)],$$

where the function $T(\tilde{E})$ is derived in Appendix II.

Finally, the zeroth order (i.e. unperturbed) part of the time function obeys Kepler's equation:

$$t_0(\tilde{E}) = \frac{h_0^3}{(1-e_0^2)^{3/2}}[T_{kep}(\tilde{E}) - T_{kep}(\tilde{E}_0)],$$

where

$$T_{kep}(\tilde{E}) = \tilde{E} - e_0 \sin\tilde{E}.$$

3.3 Variability of the parameter ϵ

The variability of the parameter ϵ for Earth and interplanetary orbits is plotted in Fig. 1 considering different values of the tangential accelerations ranging from 50 to 400 mN/tonne. In general the parameter ϵ is much smaller in Earth orbit than in interplanetary space, meaning that interplanetary orbits are more difficult to propagate analytically. Low thrust orbit transfer beyond Mars with tangential acceleration exceeding 100 mN/tonne would in general be difficult to reproduce with the current analytical solution. Yet, due to the rapid decrease of the available solar energy, such case would imply the use of nuclear electric propulsion, a space technology which has not yet been developed. On the other hand, when considering trajectories to the inner planets the higher value of the local solar gravity helps reducing ϵ so that accurate analytical propagations can be obtained. An example of low thrust interplanetary transfer to Mercury is reported later on.

4 Rectification

By comparison with an accurate numerical solution one can see that as long as the parameter epsilon remains small the above formulas represent fairly accurately the system dynamics along at least one revolution. Depending on the value of ϵ, for the multiple-revolution case,

the accuracy of the analytical representation will start to deteriorate for large θ and this will occur the earlier the larger e. In order to overcome this limitation the analytical expressions needs to be updated along the trajectory by referring, at each step, to an updated value of the dimensionless angular momentum h_0 and eccentricity e_0. When doing this a complication arises due to the fact that, in general, the osculating ellipse at the update point has undergone a precession of its apses line which makes the new initial value of the orbital parameter q_{20} (Eq. 3) different from zero. Yet the previously derived analytical formulas for the evolution of q_1, q_2, q_3, are based on the fact that $q_{20} = 0$ which greatly simplifies the analytical integration process. To overcome this difficulty a change of variable is performed which allows the previous formulas to be used. The procedure is described in the following.

Let us suppose that at the angular position $\hat{\theta}$ we want to reset the propagation. The starting orbit will be characterized by a new value of the eccentricity $\hat{e}$, angular momentum $\hat{h}$, and eccentricity vector rotation $\hat{\Delta\gamma}$. We then introduce the new variables:

$$\theta' = \theta - \hat{\Delta\gamma} \tag{33}$$

$$\Delta\gamma' = \Delta\gamma - \hat{\Delta\gamma} \tag{34}$$

$$q_1' = \frac{e}{h}\cos\Delta\gamma' \tag{35}$$

$$q_2' = \frac{e}{h}\sin\Delta\gamma' \tag{36}$$

$$q_3' = 1/h \tag{37}$$

At the beginning of the new propagation step, that is when the value of θ' is given by:

$$\theta_0' = \hat{\theta} - \hat{\Delta\gamma},$$

we have

$$\Delta\gamma' = \Delta\gamma(\theta = \hat{\theta}) - \hat{\Delta\gamma} = 0,$$

so that the initial value for the new generalized orbital elements has the same structure as found in Eqs. (18–20):

$$q_1'(\theta_0') = \frac{\hat{e}}{\hat{h}}, \tag{38}$$

$$q_2'(\theta_0') = 0, \tag{39}$$

$$q_3'(\theta_0') = \frac{1}{\hat{h}}, \tag{40}$$

and the q_i' can be propagated with the previously derived formulas to yield (Fig.

$$q_1' = \frac{\hat{e}}{\hat{h}} + \frac{\epsilon\hat{h}^3}{(1-\hat{e}^2)^2}[Q_{11}(\hat{e},\theta') - Q_{11}(\hat{e},\theta_0')],$$

$$q_2' = \frac{\epsilon\hat{h}^3}{(1-\hat{e}^2)^{3/2}}[Q_2(\hat{e},\theta') - Q_2(\hat{e},\theta_0')],$$

$$q_3' = \frac{1}{\hat{h}} + \frac{\epsilon\hat{h}^3}{(1-\hat{e}^2)^2}[Q_3(\hat{e},\theta') - Q_3(\hat{e},\theta_0')].$$

Finally, we can transfer back to the main variables $q_1, \ldots, q_3$ using the transformation:

$$\begin{pmatrix} q_1(\theta) \\ q_2(\theta) \\ q_3(\theta) \end{pmatrix} = \begin{bmatrix} \cos\hat{\Delta\gamma} & -\sin\hat{\Delta\gamma} & 0 \\ \sin\hat{\Delta\gamma} & \cos\hat{\Delta\gamma} & 0 \\ 0 & 0 & 1 \end{bmatrix} \begin{pmatrix} q_1'(\theta - \hat{\Delta\gamma}) \\ q_2'(\theta - \hat{\Delta\gamma}) \\ q_3'(\theta - \hat{\Delta\gamma}) \end{pmatrix},$$

which follows from Eqs. (34–37).

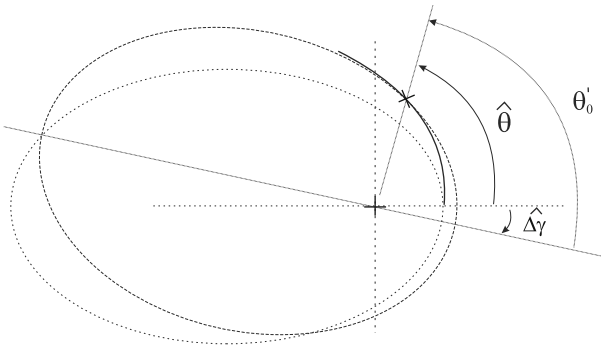

Fig. 2 Schematic of analytical recti cation. The instantaneous trajectory is denoted with a *solid line*. The *dash-dot line* ellipse represents the initial osculating orbit which is propagated analytically up to $\theta = \hat{\theta}$ where the new osculating orbit is the *dash line ellipse*. A change of variable (Eqs 33–37) is necessary to compensate for the accumulated apses line rotation $\hat{\Delta}\gamma$

For weakly perturbed orbits (say $\epsilon < 1 \times 10^{-2}$) suf cient accuracy can be obtained with one update per revolution. By performing the update a few times per revolution it will then be possible to achieve high accuracy even for higher value of the parameter epsilon (say $\epsilon < 1 \times 10^{-1}$). As the value of ϵ becomes excessively high, the number of required update points will make the analytical method more similar to a numerical propagation scheme hence diminishing its appeal.

5 Results

Simulations have been run to compare the analytical formulas with an accurate numerical integration. We have considered two test cases: a low-thrust spiral out maneuver from a geostationary transfer orbit to Earth escape and an interplanetary low-thrust trajectory from Earth to Mercury. In addition, we present the derivation of a simple formula to compute the variation of the argument of pericenter of an elliptic orbit following a 180 degree low-thrust arc. It can be interesting to evaluate the effectiveness of such maneuver during or after orbit insertion of a planetary orbiter whose argument of pericenter needs to be adjusted to a desired value. Finally, we discuss the bene t of the proposed analytical method in terms of computational time savings when compared with numerical integration.

5.1 GTO to Earth escape

For the rst test case we consider a spacecraft in a earth geostationary transfer orbit of eccentricity $e_0 = 0.72$ and initial semimajor axis of 24000 km, subject to a continuous and constant tangential acceleration $A_t = 100$ mN/tonne and neglecting other perturbative accelerations.[3] Assuming the orbit transfer starts at pericenter the corresponding dimensionless angular momentum is $s_0 = \sqrt{1 + e_0} \approx 1.3$ while the dimensionless tangential acceleration is $\epsilon = A_t / g_0 \approx 1.13 \times 10^{-5}$,where $g_0 \approx 8.28\,\mathrm{m/s^2}$ is the local gravitational acceleration at the beginning of the orbit raising maneuver.

A rst numerical comparison has been conducted in order to check the degree of convergence of the proposed analytical solution without updating the initial conditions at intermediate steps. Figure 3 plots the analytical and numerical solution for the evolution of the eccentricity over 100 orbital revolutions. A very good match is retained throughout until 20–30 orbits when the analytical solution starts diverging mostly due to the decreasing value

[3] The same example is reported on page 248 of Kemble (2006).

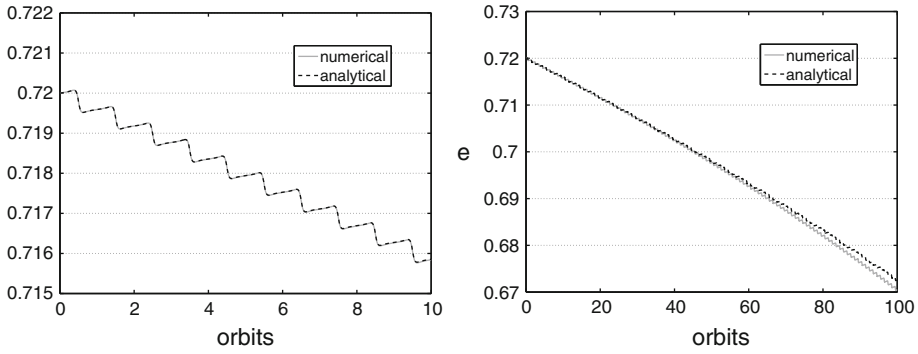

Fig. 3 Comparison between analytical and numerical solution for the evolution of the eccentricity in a GTO orbit raising maneuver

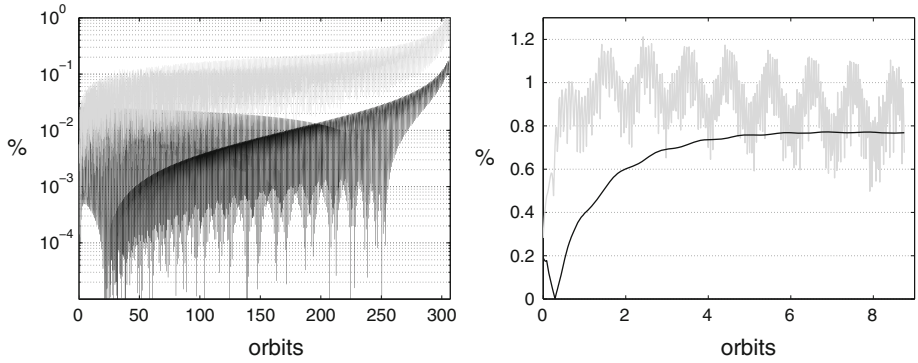

Fig. 4 Percentage of phasing (*dark*) and position error (*grey*) of the analytical solution for the GTO orbit raising (*left*) and the Mercury transfer (*right*)

of the local gravity as the orbit apoapsis increases. Note that because the eccentricity increases around periapsis but decreases to a major extent around apoapsis a net decrease in eccentricity is obtained until almost escape conditions where the eccentricity rapidly increases toward unity. By employing an optimized (non-tangential) thrust direction one would take advantage of the high initial eccentricity to escape much more quickly while avoiding the orbit eccentricity to decrease too much throughout the maneuver.

A much more accurate solution can be obtained by performing analytical recti cation. By doing this twice per orbital revolution a very good match between the analytical and numerical solution is obtained up to almost escape conditions as plotted in Fig. 5. The corresponding percentage position and phasing error as a function of the angular position are plotted in Fig. 4.

5.2 Earth to mercury

For the second test case we consider a 35-months low-thrust orbit transfer from Earth to Mercury employing a constant and continuous thrust $A_t = 200$ mN/tonne. For simplicity the Earth and Mercury orbits are considered coplanar and circular. To make the trajectory more realistic, a launch ΔV of 2 km/s in the inward radial direction is applied to the spacecraft in

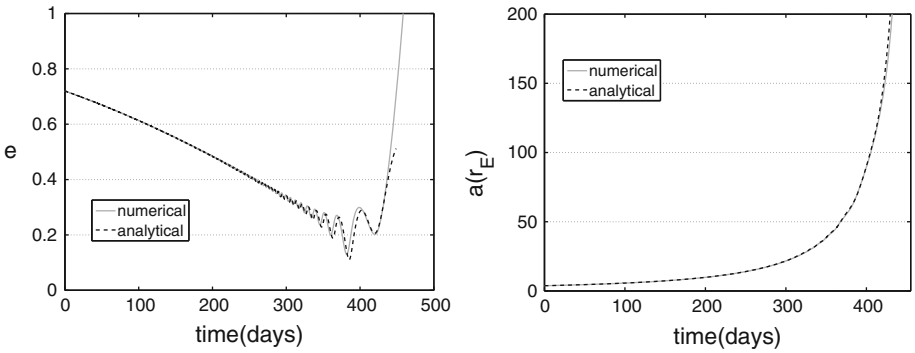

Fig. 5 Comparison between analytical and numerical solution for an orbit raising maneuver from GTO to earth escape. The plotted quantities are the orbit eccentricity (*left*) and semimajor axis (*right*). The analytical formulas are propagated twice per orbital revolution

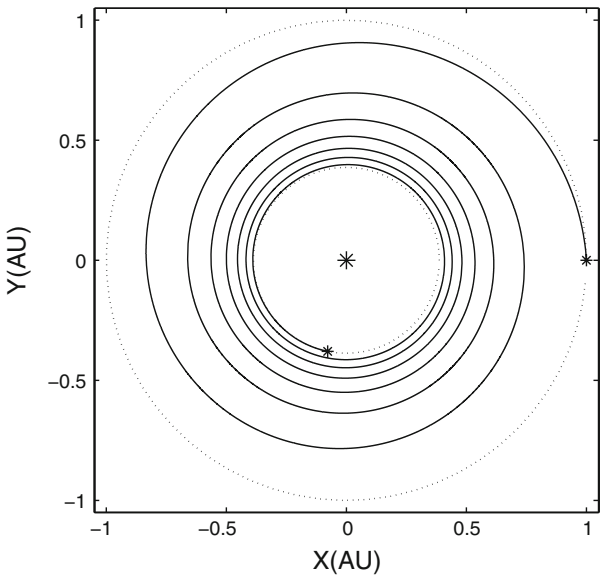

Fig. 6 Low thrust Earth–Mercury orbit transfer. Planets orbits are assumed coplanar and circular for simplicity. The small difference between the numerical and analytical trajectory cannot be appreciated from this plot

order to arrive at Mercury with almost zero relative velocity. This results in an initial eccentricity $e_0 \simeq 0.067$ while the initial dimensionless angular momentum is $h_0 = 1$. The dimensionless tangential acceleration is $\varepsilon = A_t/g_0 \approx -3.37 \times 10^{-2}$, where $g_0 \approx 0.0059\,\mathrm{m/s^2}$ is the sun gravitational acceleration at 1 AU. The interplanetary trajectory is depicted in Fig. 6 while a comparison between numerical and analytical solution is presented in Fig. 7. Due to the much higher value of epsilon, compared with the previous case, the analytical formulas have been propagated three times per revolution in order to achieve sufficient accuracy. In this way both the position and phasing error can be kept below 2% (Fig. 4).

Note that in a real mission scenario the need to perform a plane change maneuver severely complicates the trajectory design problem introducing thrust arcs with time-varying in- and out-of-plane thrust components. While the current model is clearly not suitable to describe these types of trajectories an attempt to extend its capability to the three-dimensional case will be conducted in the future.

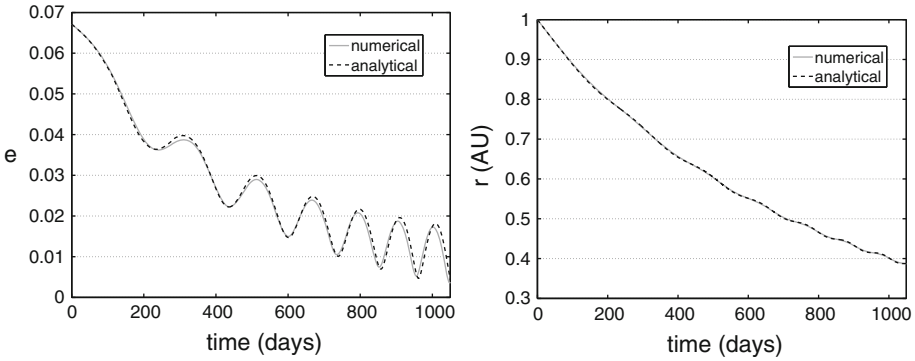

Fig. 7 Comparison between analytical and numerical solution for an Earth to Mercury transfer. The analytical formulas are here recti ed three times per orbital revolution

5.3 Variation of argument of periapsis over a continuous thrust arc

Let our spacecraft be located at initial radius r_0 and angular distance θ_0 from the pericenter of an elliptic orbit with initial eccentricity e_0. Let us apply a continuous and constant tangential thrust acceleration of magnitude A_t along the arc $[\theta_0, \theta]$. The corresponding value of the parameter ϵ is given by Eq. (15).

The variation of the argument of periapsis across the thrust arc is just the rotation $\Delta\gamma$ of the eccentricity vector around the angular momentum direction. The rst order solution is (Eq. 41):

$$\Delta\gamma \simeq \tan^{-1}\left(\frac{q_{20}+\epsilon q_{21}}{q_{10}+\epsilon q_{11}}\right) = \tan^{-1}\left(\frac{\epsilon q_{21}}{e_0/h_0+\epsilon q_{11}}\right) \approx \frac{\epsilon h_0 q_{21}}{e_0}. \tag{41}$$

where, following Eq. (27) and Eq. (47) in Appendix I we have:

$$q_{21} = \frac{h_0^3}{(1-e_0^2)^{3/2}}[Q_{21}(e_0,\tilde{E}) - Q_{21}(e_0,\tilde{E}_0)],$$

$$Q_{21}(e_0,\tilde{E}) = -\frac{2}{e_0}\left[\tan^{-1}\left(\frac{e_0\cos\tilde{E}}{\sqrt{1-e_0^2\cos^2\tilde{E}}}\right) + \sqrt{1-e_0^2\cos^2\tilde{E}}\right].$$

Here $\tilde{E}_0$ and $\tilde{E}$ are related to θ_0 and θ through Eq. (22), while h_0 can be computed through Eq. (1).

For the particular case in which the thrust is applied over an arc from -180 to 0 degree we have:

$$\tilde{E}_0 = \theta_0 = -\pi; \quad \tilde{E} = \theta = 0,$$

and the above formulas yield:

$$\Delta\gamma[-\pi, 0] \simeq \frac{4A_t r_0^2\sqrt{1-e_0}}{\mu e_0^2(1+e_0)^{3/2}}\tan^{-1}\left(\frac{e_0}{\sqrt{1-e_0^2}}\right). \tag{42}$$

Table 1 CPU-time comparison for the GTO orbit raising problem

Orbits	Numerical (s)	Analytical (s)
300	35	0.33
150	21	0.20
75	14	0.14

5.4 Computation time savings

A key advantage of the proposed method is the potential computation time savings when compared to numerical integration. Among the different possible approaches that can be used we have chosen to compare the two methods based on the computation time (CPU-time) required for the two examples shown above and with comparable position accuracy. To this end we implemented a numerical integration method of the tangential thrust problem using the Peláez formulation[4] and employing the 5th order Dorman–Prince numerical integrator corresponding to the Matlab ode45 subroutine. The integration tolerances were chosen such as to provide an integration error roughly equal to the one provided by the analytical method for the two test cases considered. The numerical and analytical method were both implemented in Matlab and the results of the comparison for the GTO orbit raising problem are listed in Table 1. A one order of magnitude computation savings can be obtained with the analytical method proposed almost independently of the number of revolutions. Similar results are obtained for the Earth to Mercury transfer.

It must be stressed that the one presented here is just a preliminary comparison analysis. An extensive comparison, which goes beyond the scope of the present article, should consider a higher number of test cases, different integrators and a more appropriate Fortran or C++ implementation.

6 Conclusions

A new asymptotic solution for the two-body problem perturbed by constant tangential acceleration has been provided with the aid of a special perturbation formulation of the orbit equations of motion. Relatively compact analytical formulas accurately represent the trajectory evolution in time accounting for both secular and oscillatory variations of the orbital elements and are not limited by high values of the orbit eccentricity. The accuracy of the method has been tested with highly eccentric Earth orbits evolving beyond lunar distance and interplanetary orbits to the inner solar system planets referring to tangential acceleration magnitude achievable by state-of-the-art electric propulsion engines. It is seen that for small values (say $\epsilon < 1 \times 10^{-4}$) of the non-dimensional acceleration magnitude, as it is the case in Low Earth Orbit, the approximate analytical solution can be used to accurately represent the orbit evolution along very large intervals without iterating the process. For the worst case scenario in which the acceleration magnitude is high compared to local gravity, which is the case of interplanetary orbits, high accuracy can be retained by updating the values of the initial generalized parameters a few times along each orbit. A preliminary estimation suggests that a computation time savings of about one order of magnitude can be obtained

[4] This formulation was seen to provide the highest performance in terms of accuracy vs computation time when compared with regularized two-body problem formulations such as the Kustaanheimo–Stiefel (Peláez et al. 2007)

when comparing the proposed solution with very fast numerical integration of comparable accuracy.

Future work will address the more general problem in which the tangential acceleration is not constant along the orbit and the extension of the method to non-planar trajectories.

Acknowledgments The work was supported by the DGI of the Spanish Ministry of Education and Science under the research grant "Dynamical Simulations of Complex Space Systems" contract number AYA2010-18796. The author would like to thank the two reviewers for their precious comments and Dr. Rüdiger Jehn from ESA-ESOC for his interesting suggestions.

Appendix I

The differential Eqs. (23–25) associated to the first order variation of q_{i1} can be solved by quadrature and put in the form:

$$q_{11}(\tilde{E}) - q_{11}(\tilde{E}_0) = \frac{h_0^3}{(1-e_0^2)^2}[Q_{11}(\tilde{E}) - Q_{11}(\tilde{E}_0)], \tag{43}$$

$$q_{21}(\tilde{E}) - q_{21}(\tilde{E}_0) = \frac{h_0^3}{(1-e_0^2)^{3/2}}[Q_{21}(\tilde{E}) - Q_{21}(\tilde{E}_0)], \tag{44}$$

$$q_{31}(\tilde{E}) - q_{31}(\tilde{E}_0) = \frac{h_0^3}{(1-e_0^2)^2}[Q_{31}(\tilde{E}) - Q_{31}(\tilde{E}_0)], \tag{45}$$

where

$$Q_{11}(\tilde{E}) = \int_0^{\tilde{E}} \frac{e_0(e_0^2-2)\cos^2\tilde{E} + 2\cos\tilde{E} - e_0}{\sqrt{1-e_0^2\cos^2\tilde{E}}} d\tilde{E} \tag{46}$$

$$Q_{21}(\tilde{E}) = \int_0^{\tilde{E}} \frac{2\sin\tilde{E}(1-e_0\cos\tilde{E})}{\sqrt{1-e_0^2\cos^2\tilde{E}}} d\tilde{E} \tag{47}$$

$$Q_{31}(\tilde{E}) = \int_0^{\tilde{E}} -\frac{(1-e_0\cos\tilde{E})^2}{\sqrt{1-e_0^2\cos^2\tilde{E}}} d\tilde{E} \tag{48}$$

The above integrals can be solved analytically and can be conveniently written separating a secular and oscillatory component:

$$Q_{i1}(\tilde{E}) = Q_{i1,sec}(\tilde{E}) + Q_{i1,osc}(\tilde{E}).$$

The secular terms yield:

$$Q_{11,sec}(\tilde{E}) = k_1\tilde{E}$$
$$Q_{21,sec}(\tilde{E}) = 0$$
$$Q_{31,sec}(\tilde{E}) = k_3\tilde{E}$$

where k_1 and k_3 are given by:

$$k_1 = \frac{2\mathcal{E}(e_0)(2-e_0^2) - 4\mathcal{K}(e_0)}{\pi e_0}$$
$$k_3 = \frac{2\mathcal{E}(e_0) - 4\mathcal{K}(e_0)}{\pi}$$

with $\mathcal{K}$ and $\mathcal{E}$ indicating complete elliptic integrals of the first and second kind, respectively:

$$\mathcal{K}(e_0) = \int_0^1 \frac{dz}{\sqrt{(1-z^2)(1-e_0^2 z^2)}}$$
$$\mathcal{E}(e_0) = \int_0^1 \sqrt{\frac{1-e_0^2 z^2}{1-z^2}}\, dz$$

The oscillatory terms are periodic functions of period 2π and can be written for $-\pi < \tilde{E} < \pi$ as:

$$Q_{11,osc}(\tilde{E}) = \frac{\sin\tilde{E}}{\left|\sin\tilde{E}\right|} \times \frac{1}{e_0}\Bigg[2\mathcal{F}(\cos\tilde{E}, e_0) - (2-e_0^2)\mathcal{E}(\cos\tilde{E}, e_0) - 2\mathcal{K}(e_0) + (2-e_0^2)\mathcal{E}(e_0)$$
$$- \ln\left((1-e_0)^{-1}\left(1 - 2e_0^2\cos^2\tilde{E} + e_0^2 - 2e_0\left|\sin\tilde{E}\right|\sqrt{1-e_0^2\cos^2\tilde{E}}\right)\right)\Bigg] - k_1\tilde{E}$$
$$Q_{21,osc}(\tilde{E}) = -\frac{2}{e_0}\left[\tan^{-1}\left(\frac{e_0\cos\tilde{E}}{\sqrt{1-e_0^2\cos^2\tilde{E}}}\right) + \sqrt{1-e_0^2\cos^2\tilde{E}}\right]$$
$$Q_{31,osc}(\tilde{E}) = \frac{\sin\tilde{E}}{\left|\sin\tilde{E}\right|} \times \Bigg[2\mathcal{F}(\cos\tilde{E}, e_0) - \mathcal{E}(\cos\tilde{E}, e_0) - 2\mathcal{K}(e_0) + \mathcal{E}(e_0)$$
$$- \ln\left((1-e_0)^{-1}\left(1 - 2e_0^2\cos^2\tilde{E} + e_0^2 - 2e_0\left|\sin\tilde{E}\right|\sqrt{1-e_0^2\cos^2\tilde{E}}\right)\right)\Bigg] - k_3\tilde{E}$$

where $\mathcal{F}(\cos\tilde{E}, e_0)$ and $\mathcal{E}(\cos\tilde{E}, e_0)$ are *incomplete* elliptic integrals of the first and second kind, respectively:

$$\mathcal{F}(\cos\tilde{E}, e_0) = \int_0^{\cos\tilde{E}} \frac{dz}{\sqrt{(1-z^2)(1-e_0^2 z^2)}}$$
$$\mathcal{E}(\cos\tilde{E}, e_0) = \int_0^{\cos\tilde{E}} \sqrt{\frac{1-e_0^2 z^2}{1-z^2}}\, dz$$

The oscillatory terms can be expanded in Taylor series for small e_0 and written in the compact matrix form:

$$Q_{11,osc}(\tilde{E}) = (\mathcal{Q}_1 \boldsymbol{v}_{e0})^T \boldsymbol{v}_S$$
$$Q_{21,osc}(\tilde{E}) = (\mathcal{Q}_2 \boldsymbol{v}_{e0})^T \boldsymbol{v}_C$$
$$Q_{31,osc}(\tilde{E}) = (\mathcal{Q}_3 \boldsymbol{v}_{e0})^T \boldsymbol{v}_S$$

where

$$\boldsymbol{v}_{e0} = \left(1, e_0, e_0^2, e_0^3 \ldots\right)^T$$

$$\boldsymbol{v}_S = \left(\sin\tilde{E}, \sin 2\tilde{E}, \sin 3\tilde{E}, \ldots\right)^T$$

$$\boldsymbol{v}_C = \left(\cos\tilde{E}, \cos 2\tilde{E}, \cos 3\tilde{E}, \ldots\right)^T$$

$$\mathcal{Q}_1 = \begin{bmatrix} 2 & 0 & 3/4 & 0 & 15/32 & \ldots \\ 0 & -1/2 & 0 & -1/8 & 0 & \ldots \\ 0 & 0 & 1/12 & 0 & 5/64 & \ldots \\ 0 & 0 & 0 & -1/32 & 0 & \ldots \\ 0 & 0 & 0 & 0 & 3/320 & \ldots \\ \vdots & \vdots & \vdots & \vdots & \vdots & \ddots \end{bmatrix}$$

$$\mathcal{Q}_2 = \begin{bmatrix} -2 & 0 & -1/4 & 0 & -3/32 & \ldots \\ 0 & 1/2 & 0 & 1/8 & 0 & \ldots \\ 0 & 0 & -1/12 & 0 & -3/64 & \ldots \\ 0 & 0 & 0 & 1/32 & 0 & \ldots \\ 0 & 0 & 0 & 0 & -3/320 & \ldots \\ \vdots & \vdots & \vdots & \vdots & \vdots & \ddots \end{bmatrix}$$

$$\mathcal{Q}_3 = \begin{bmatrix} 0 & 2 & 0 & 3/4 & 0 & \ldots \\ 0 & 0 & -3/8 & 0 & -7/32 & \ldots \\ 0 & 0 & 0 & 1/12 & 0 & \ldots \\ 0 & 0 & 0 & 0 & -7/256 & \ldots \\ 0 & 0 & 0 & 0 & 0 & \ldots \\ \vdots & \vdots & \vdots & \vdots & \vdots & \ddots \end{bmatrix}$$

Appendix II

The first order differential equations for the variation of t_1 in terms of the variable $\tilde{E}$ is:

$$\frac{dt_1}{d\tilde{E}} = \frac{3e_0 - (2 + 2e_0^2)\cos\tilde{E} + e_0\cos 2\tilde{E}}{q_{30}^4(1-e_0^2)^{5/2}} q_{11}(\tilde{E}) - \frac{2\sin\tilde{E} - e_0\sin 2\tilde{E}}{q_{30}^4(1-e_0^2)^2} q_{21}(\tilde{E}) - \frac{3 - (5e_0 - e_0^3)\cos\tilde{E} + e_0^2\cos 2\tilde{E}}{q_{30}^4(1-e_0^2)^{5/2}} q_{31}(\tilde{E})$$

which can be integrated after considering the previously derived expansion of the $q_{i1}(\tilde{E})$. The complete solution of the integral is:

$$t_1(e_0, \tilde{E}) = \frac{h_0^7}{(1-e_0^2)^{9/2}}\left[T(\tilde{E}) - T(\tilde{E}_0)\right],$$

where

$$T(\tilde{E}) = \int_0^{\tilde{E}} \left[3e_0 - (2+2e_0^2)\cos\tilde{E} + e_0\cos 2\tilde{E}\right]\left[Q_1(\tilde{E}) - Q_1(\tilde{E}_0)\right] + \left[(1-e_0^2)(-2\sin\tilde{E} + e_0\sin 2\tilde{E})\right]\left[Q_2(\tilde{E}) - Q_2(\tilde{E}_0)\right] + \left[-3 + (5e_0 - e_0^3)\cos\tilde{E} - e_0^2\cos 2\tilde{E}\right]\left[Q_3(\tilde{E}) - Q_3(\tilde{E}_0)\right] d\tilde{E}$$

Again, the function T can be expressed as a sum of secular and oscillatory terms:

$$T(\tilde{E}) = T_{sec}(\tilde{E}) + T_{osc}(\tilde{E}).$$

The *secular* part yields:

$$T_{sec}(\tilde{E}) = \frac{3}{2}(k_1 e_0 - k_3)\,\tilde{E}^2 + \tilde{E}\left[\left(k_3 e_0(5-e_0^2) - 2k_1(1+e_0^2)\right)\sin\tilde{E} + \frac{1}{2}e_0(k_1 - k_3 e_0)\sin 2\tilde{E} + g(e_0, \tilde{E}_0)\right]$$

where

$$g(e_0, \tilde{E}_0) = (\boldsymbol{G}\boldsymbol{v}_{e0})^T\,\boldsymbol{w}_{S0}$$

with

$$\boldsymbol{w}_{S0} = \left(1, \sin\tilde{E}_0, \sin 2\tilde{E}_0, \sin 3\tilde{E}_0, \ldots\right)^T,$$

and

$$\boldsymbol{G} = \begin{bmatrix} 3k_3\tilde{E}_0 & -3k_1\tilde{E}_0 & 0 & 0 & 0 & \ldots \\ 0 & 0 & 0 & 0 & 0 & \ldots \\ 0 & 0 & 3/8 & 0 & -9/32 & \ldots \\ 0 & 0 & 0 & 0 & 0 & \ldots \\ 0 & 0 & 0 & 0 & 3/256 & \ldots \\ \vdots & \vdots & \vdots & \vdots & \vdots & \ddots \end{bmatrix}$$

Finally, the *oscillatory* part yields:

$$T_{,osc}(\tilde{E}) = (\boldsymbol{H}\boldsymbol{v}_{e0})^T\,\boldsymbol{v}_C + p_1\cos\tilde{E} + p_2\sin\tilde{E} + p_3\cos 2\tilde{E} + p_4\sin 2\tilde{E}$$

where

$$\boldsymbol{H} = \begin{bmatrix} 4-2k_1 & 5k_3 & -2k_1 - 10/3 & -k_3 - 5/24 & -11/30 \\ 0 & k_1/4 - 1 & -k_3/4 + 13/48 & 5/6 & -17/192 \\ 0 & 0 & 0 & -1/8 & 0 \\ 0 & 0 & 0 & 0 & 317/15360 \\ 0 & 0 & 0 & 0 & 0 \end{bmatrix}$$

and

$$p_1 = (\boldsymbol{P}_1\boldsymbol{v}_{e0})^T\,\boldsymbol{v}_{C0}$$
$$p_2 = (\boldsymbol{P}_2\boldsymbol{v}_{e0})^T\,\boldsymbol{v}_{S0}$$
$$p_3 = (\boldsymbol{P}_3\boldsymbol{v}_{e0})^T\,\boldsymbol{v}_{C0}$$
$$p_4 = (\boldsymbol{P}_4\boldsymbol{v}_{e0})^T\,\boldsymbol{v}_{S0}$$

with

$$\boldsymbol{P}_1 = \begin{bmatrix} -4 & 1 & 10/3 & -\frac{11}{16} & \frac{11}{30} & -\frac{5}{16} \\ 4 & 0 & -7/2 & 0 & -\frac{5}{16} & 0 \\ 0 & -1 & 0 & 3/4 & 0 & 1/4 \\ 0 & 0 & 1/6 & 0 & -\frac{7}{96} & 0 \\ 0 & 0 & 0 & -1/16 & 0 & 1/16 \\ 0 & 0 & 0 & 0 & \frac{3}{160} & 0 \end{bmatrix}$$

$$\boldsymbol{P}_2 = \begin{bmatrix} 2k_1\tilde{E}_0 & -5k_3\tilde{E}_0 & 2k_1\tilde{E}_0 & k_3\tilde{E}_0 & 0 & 0 \\ 4 & 0 & -9/2 & 0 & \frac{11}{16} & 0 \\ 0 & -1 & 0 & 5/8 & 0 & \frac{15}{32} \\ 0 & 0 & 1/6 & 0 & -\frac{3}{32} & 0 \\ 0 & 0 & 0 & -1/16 & 0 & \frac{19}{256} \\ 0 & 0 & 0 & 0 & \frac{3}{160} & 0 \end{bmatrix}$$

$$\boldsymbol{P}_3 = \begin{bmatrix} 0 & 1 & -1/4 & -5/6 & \frac{11}{64} & -\frac{11}{120} \\ 0 & -1 & 0 & \frac{7}{8} & 0 & \frac{5}{64} \\ 0 & 0 & 1/4 & 0 & -3/16 & 0 \\ 0 & 0 & 0 & -1/24 & 0 & \frac{7}{384} \\ 0 & 0 & 0 & 0 & \frac{1}{64} & 0 \\ 0 & 0 & 0 & 0 & 0 & -\frac{3}{640} \end{bmatrix}$$

$$\boldsymbol{P}_4 = \begin{bmatrix} 0 & -\frac{k_1\tilde{E}_0}{2} & \frac{k_3\tilde{E}_0}{2} & 0 & 0 & 0 \\ 0 & -1 & 0 & 5/8 & 0 & \frac{9}{64} \\ 0 & 0 & 1/4 & 0 & -1/8 & 0 \\ 0 & 0 & 0 & -1/24 & 0 & \frac{1}{384} \\ 0 & 0 & 0 & 0 & \frac{1}{64} & 0 \\ 0 & 0 & 0 & 0 & 0 & -\frac{3}{640} \end{bmatrix}$$

References

Battin, R.: An introduction to the mathematics and methods of astrodynamics. AIAA Education Series. American Institute of Aeronautics and Astronautics Inc., New York (1999)

Benney, D.: Escape from a circular orbit using tangential thrust. Jet Propul. **28**(3), 167–169 (1958)

Boltz, F.: Orbital motion under continuous tangential thrust. J. Guid. Control Dyn. **15**, 1503–1507 (1992)

Gao, Y., Kluever, C.: Analytic orbital averaging technique for computing tangential-thrust trajectories. J. Guid. Control Dyn. **28**(6), 1320–1323 (2005)

Kechichian, J.: Orbit raising with low-thrust tangential acceleration in presence of Earth shadow. J. Spacecr. Rockets **35**(4), 516–525 (1998)

Kemble, S.: Interplanetary mission analysis and design. Springer, Berlin (2006)

Kevorkian, J., Cole, J., John, F.: Perturbation Methods in Applied Mathematics, vol. 34. Springer, New York (1981)

Peláez, J., Hedo, J., de Andrés, P.R.: A special perturbation method in orbital dynamics. Celest. Mech. Dyn. Astron. **97**(2), 131–150 (2007)

Waldvogel, J.: Quaternions for regularizing celestial mechanics: the right way. Celest. Mech. Dyn. Astron. **102**(1), 149–162 (2008)